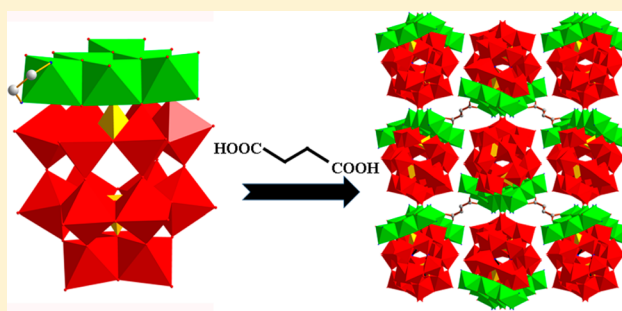


Planar $\{\text{Ni}_6\}$ Cluster-Containing Polyoxometalate-based Inorganic–Organic Hybrid Compound and Its Extended StructureXingquan Wang,[†] Shuxia Liu,^{*,†} Yiwei Liu,[†] Danfeng He,[†] Ning Li,[†] Jun Miao,[†] Yujuan Ji,[†] and Guoyu Yang^{*,‡}[†]Key Laboratory of Polyoxometalate Science of the Ministry of Education, College of Chemistry, Northeast Normal University, Changchun, Jilin 130024, China[‡]State Key Laboratory of Structural Chemistry, Fujian Institute of Research on the Structure of Matter, Chinese Academy of Sciences, Fuzhou, Fujian 350002, China

Supporting Information

ABSTRACT: Two $\{\text{Ni}_6\}$ cluster-containing inorganic–organic hybrid compounds have been successfully synthesized in the presence of organic amine under hydrothermal conditions, and they were characterized by powder and single-crystal X-ray diffraction, elemental analysis, thermogravimetric analysis, and IR spectroscopy. Structural analysis indicates that $[\text{Ni}_{0.5}(\text{H}_2\text{O})_3][\{\text{Ni}_6(\mu_3\text{-OH})_3\text{en}(\text{H}_2\text{O})_{10}\}(\text{H}_2\text{P}_2\text{W}_{15}\text{O}_{56})] \cdot 10\text{H}_2\text{O}$ (**1**, en = ethylenediamine) is a triangular inorganic $\{\text{Ni}_6\}$ cluster substituted polyoxotungstate with only one en to stabilize the $\{\text{Ni}_6\}$ cluster. However, $[\text{Ni}(\text{dap})_2][\{\text{Ni}_{1.5}(\text{dap})_{1.5}(\text{H}_2\text{O})_3[\text{Ni}_6(\mu_3\text{-OH})_3(\text{dap})_2(\text{en})(\text{H}_2\text{O})\{\text{O}_2\text{C}(\text{CH}_2)_2\text{CO}_2\}_{0.5}(\text{CH}_3\text{COO})(\text{P}_2\text{W}_{15}\text{O}_{56})]\} \cdot 15\text{H}_2\text{O}$ (**2**, dap = 1,2-diaminopropane) is a three-dimensional inorganic–organic hybrid compound linked by succinic acid. The magnetic properties of both compounds were studied. In addition, the adsorption properties of compound **2** have also been investigated.



INTRODUCTION

The inorganic–organic hybrid materials have been studied extensively for their potential applications in the fields of catalysis, liquid crystals, magnetism, and photochemistry.^{1–6} Moreover, these hybrid materials could also combine the advantages of individual inorganic and organic components together.^{7–9} Thus, it is very meaningful to synthesize functional inorganic–organic hybrid materials. The critical step for the preparation of such hybrid materials is to choose the appropriate organic and inorganic components. Polyoxometalates (POMs) are a remarkable class of inorganic metal oxide clusters with varieties of structures and rich electronic properties.^{10–17} They can react with organic groups by weak forces including electrostatic interactions and van der Waals force to form a variety of supramolecular compounds.^{18–21} Thus, they are the best candidates for the inorganic component of such hybrid materials. However, compared with saturated POMs, lacunary POMs have high negative charges and exhibit strong coordination ability by exposing more active coordination sites.^{22,23} As a result, lacunary POMs of the Keggin and Dawson type usually act as excellent inorganic building units coordinating with the transition-metal (TM) ions to form varieties of transition-metal-substituted POMs (TMSPs).^{24–31} Furthermore, the oxygen atoms on the transition metal are very active, which can be replaced by the organic components to form various inorganic–organic hybrid materials.^{31–36} These hybrids are more stable than those compounds formed by

electrostatic interactions between cationic and POM anions.^{37,38}

As we all know, most of the transition metals usually show a paramagnetic behavior because of their unpaired electron. Gathering the transition metal into clusters is very important in the magnetic field. Recently, more and more people focus their attention on the lacunary POMs, because the lacunary POMs possess high reaction activity and can serve as multidentate ligand to promote the formation of transition-metal clusters. To date, numerous POMs with transition-metal clusters have been reported, such as two cobalt-based single molecule magnets $\{\text{Co}_{16}[\text{PW}_9]_4\}$ ³⁹ and $\{\text{Co}_{14}[\text{P}_2\text{W}_{15}]_4\}$,⁴⁰ the nickel-containing POMs $\{\text{Ni}_7[\text{SiW}_8\text{O}_{31}]_2\}$,⁴¹ $\{\text{Ni}_9[\text{PW}_9\text{O}_{34}]_3\}$,⁴² and $\{\text{Ni}_{14}[\text{P}_2\text{W}_{15}\text{O}_{56}]_4\}$,⁴³ and the copper-containing cyclic POMs $\{\text{Cu}_{20}\text{X}[\text{P}_8\text{W}_{48}\text{O}_{184}]\}$ (X = Cl, Br, I).⁴⁴ However, most of the transition-metal clusters in them are stabilized by more than one polyanion, and the synthesis of TM clusters stabilized by isolated POM fragments is still a challenge. Besides, introducing organic components into POMs or TMSPs to construct an extended structure is also difficult. In 2008, Cronin et al. introduced the $(\text{HOCH}_2)_3\text{NH-CO}-(\text{CH}_2)_{14}\text{CH}_3$ into an Anderson POM to make amphiphilic hybrids.⁴⁵ The introduction of organic components will not only obtain diverse structures but also affect the electronic structure and

Received: September 24, 2014

Published: November 26, 2014

Table 1. Crystal Data and Structural Refinement for Compounds 1 and 2

	1	2
empirical formula	C ₂ H ₅₉ N ₂ O ₈₄ P ₂ W ₁₅ Ni _{6.5}	C _{22.5} H ₁₀₉ N ₁₃ O ₈₂ P ₂ W ₁₅ Ni _{8.5}
<i>M</i> , g/mol	4656.10	5192.28
cryst. syst.	monoclinic	monoclinic
space group	<i>P</i> 21/ <i>c</i>	<i>C</i> 2/ <i>c</i>
<i>a</i> , Å	14.8355(4)	28.5520(17)
<i>b</i> , Å	18.1052(4)	27.8454(17)
<i>c</i> , Å	28.8773(6)	27.887(2)
α , deg	90	90
β , deg	95.671(2)	120.610(10)
γ , deg	90	90
vol, Å ³	7718.5(3)	19082(2)
crystal size, mm ³	0.20 × 0.15 × 0.12	0.25 × 0.18 × 0.14
<i>Z</i>	2	4
<i>D</i> _{calc} , mg/m ³	3.960	3.463
abs coeff, mm ⁻¹	23.959	19.768
θ range, deg	2.84–25.10	2.04–24.70
reflns collected	29861	47960
indep reflns	13751	16274
<i>R</i> (int)	0.0488	0.0822
GOF on <i>F</i> ²	1.013	1.036
<i>R</i> ₁ [<i>I</i> > 2 σ (<i>I</i>)] ^a	0.0455	0.0469
<i>wR</i> ₂ (all data) ^b	0.1124	0.1117

$$^a R_1 = \sum \|F_o\| - |F_c| / \sum \|F_o\|, \quad ^b wR_2 = [\sum w(F_o^2 - F_c^2)^2 / \sum w(F_o^2)^2]^{1/2}.$$

polarity of POMs. Furthermore, the introduction of organic components will also make the resulting compound porous. As a result, POM-containing inorganic–organic hybrid materials will display potential applications in shape-selective catalysis and selective adsorption.

On the basis of the aforementioned points, we choose the trivalent Dawson-type polyanion [P₂W₁₅O₅₆]¹²⁻ (abbreviated as {P₂W₁₅}) as the building unit, reacting with NiCl₂·6H₂O and the appropriate en (en = ethanediamine) in HAC-NaAc buffer solution under hydrothermal conditions, yielding a new hybrid compound: [Ni_{0.5}(H₂O)₃]{[Ni₆(μ_3 -OH)₃en(H₂O)₁₀]- (H₂P₂W₁₅O₅₆)}·10H₂O (**1**). Structure analysis indicates that **1** is one example of a triangular inorganic {Ni₆} cluster substituted polyoxotungstate based on trivalent Dawson-type POMs. Furthermore, we also attempt to introduce succinic acid into the above system aiming to design the synthesis of the multidimensional structure based on Ni₆-substituted Dawson POMs. Succinic acid is a flexible ligand with varieties of coordination modes that can coordinate with transition metals (TMs) allodially. The introduction of succinic acid in the above system may make the final hybrid materials adsorb some molecules selectively. Fortunately, after several attempts, the expected novel 3D hybrid materials [Ni(dap)₂]{[Ni_{1.5}(dap)_{1.5}(H₂O)₃][Ni₆(μ_3 -OH)₃(dap)₂(en)(H₂O) {O₂C(CH₂)₂CO₂}]_{0.5}-(CH₃COO)(P₂W₁₅O₅₆)}·15H₂O (**2**, dap = 1,2-diaminopropane) has been successfully obtained by replacing en with dap, and adding a little of succinic acid to above system. Structure analysis showed that **2** is a three-dimensional structure linked by W=O-Ni, O-Ni-O, and succinic acid linker.

EXPERIMENTAL SECTION

Materials and Methods. All chemicals were purchased from the Aldrich company and used without additional purification. The {P₂W₁₅} precursor was synthesized according to the procedure described in the literature⁴⁶ and characterized by IR spectra. Elemental analyses for C, N, and H were performed on a PerkinElmer 2400

CHN elemental analyzer and, for P, W, and Ni, were determined with a PLASMASPEC (I) ICP atomic emission spectrometer. The IR spectra in KBr pellets were recorded in the range of 400–4000 cm⁻¹ with an Alpha Centaur FT-IR spectrophotometer. Powder X-ray diffraction (XRD) measurements were performed on a Rigaku D/MAX-3 instrument with Cu-K α (λ = 1.5418 Å) radiation in the angular range 2θ = 3–60 °C at 293 K. Thermogravimetric analyses (TGA) were carried out by using a PerkinElmer TGA7 instrument, with a heating rate of 10 °C/min under a nitrogen atmosphere. The magnetic susceptibility data were obtained on a SQUID magnetometer (Quantum Design, MPMS-5) over the temperature range of 300–2 K at a magnetic field of 1000 Oe. Gas adsorption measurements were performed with a Hiden Isochema Intelligent Gravimetric Analyzer (IGA-100B).

Synthesis of Compound 1. A sample of Na₁₂[P₂W₁₅O₅₆] $\cdot n$ H₂O (0.40 g) and NiCl₂·6H₂O (0.57 g) were stirred for 10 min in a 0.25 mol/L HAC-NaAc buffer solution (pH = 4.8, 10 mL), forming a clear green solution. Then, en (0.05 mL) was added dropwise, and the solution became cloudy immediately. Then, the solution was continuously stirred for 1 h. The final solution was put into a 25 mL stainless steel reactor with a Teflon liner and heated for 3 days at 170 °C and then cooled to room temperature, upon which green block crystals of **1** were obtained by filtration, and they were washed with distilled water and air-dried. Yield: 23% (based on Ni). Elemental analysis for C₂H₅₉N₂Ni_{6.5}O₈₄P₂W₁₅ (Calc.) C 5.15, H 1.27, N 0.60, P 1.33, Ni 8.19, W 59.21 (%). (Found) C 5.11, H 1.24, N 0.56, P 1.28, Ni 8.25, W 59.27 (%).

Synthesis of Compound 2. A sample of Na₁₂[P₂W₁₅O₅₆] $\cdot n$ H₂O (0.40 g) and NiCl₂·6H₂O (0.57 g) was stirred for 10 min in a 0.5 mol/L HAC-NaAc buffer solution (pH = 4.8, 10 mL), forming a clear green solution. Then, dap (0.3 mL) was added dropwise, and the solution became cloudy immediately. After the solution was continuously stirred for 10 min, 0.10 g of succinic acid was added to the cloudy solution, and then the solution was continuously stirred for 1 h. The final solution was put into a 25 mL stainless steel reactor with a Teflon liner and heated for 3 days at 170 °C and then cooled to room temperature, upon which green block crystals of **2** were obtained by filtration, and they were washed with distilled water and air-dried. Yield: 41% (based on Ni). Elemental analysis for C_{22.5}H₁₀₉N₁₃O₈₂

$P_2W_{15}Ni_{8.5}$ (Calc.) C 5.20, H 2.10, N 3.51, P 1.19, Ni 9.61, W 53.10 (%). (Found) C 5.17, H 2.14, N 3.48, P 1.23, Ni 9.65, W 53.16 (%).

X-ray Crystallography. Single-crystal X-ray diffractometry was recorded on a Bruker Smart Apex CCD diffractometer with Mo- $K\alpha$ monochromated radiation ($\lambda = 0.71073 \text{ \AA}$) at room temperature. The linear absorption coefficients, scattering factors for the atoms, and anomalous dispersion corrections were taken from the International Tables for X-ray Crystallography.⁴⁷ Empirical absorption corrections were applied. The structures of **1** and **2** were solved by using the direct method and refined through the full-matrix least-squares method on F^2 using the SHELXS-97 crystallographic software package.⁴⁸ Anisotropic thermal parameters were used to refine all non-hydrogen atoms. Those hydrogen atoms attached to lattice water molecules were not located. Crystallization water molecules were estimated by thermogravimetry, and only partial oxygen atoms of water molecules in **2** were achieved with the X-ray structure analysis. The IR spectra of two compounds are shown in Figure S1 (Supporting Information). The experimental and simulated powder X-ray diffraction (PXRD) patterns of both compounds are shown in Figure S2 (Supporting Information). The diffraction peaks on both experimental and simulated patterns match well in position, indicating their phase purity. The crystal data and structure refinement results of **1** and **2** are summarized in Table 1. CCDC-1015463 for **1** and CCDC-1015464 for **2** contain the supplementary crystallographic data for this paper. These data can be obtained free of charge from The Cambridge Crystallographic Data Centre.

RESULTS AND DISCUSSION

Synthesis and Structure. The compound **1** was synthesized in a one-pot reaction of the trilacunary polyanion precursor $[P_2W_{15}O_{56}]^{12-}$ with $NiCl_2 \cdot 6H_2O$ and en under hydrothermal reaction. It cannot be obtained in conventional aqueous conditions. In addition, the ionic strength also affects the formation of compound **1**; the yield of **1** is reduced greatly when 0.25 mol/L HAC-NaAc buffer solution was replaced by 0.5 mol/L HAC-NaAc buffer solution. X-ray diffraction analyses reveal that **1** (Figure 1a) consists of one anion $[Ni_6(\mu_3-$

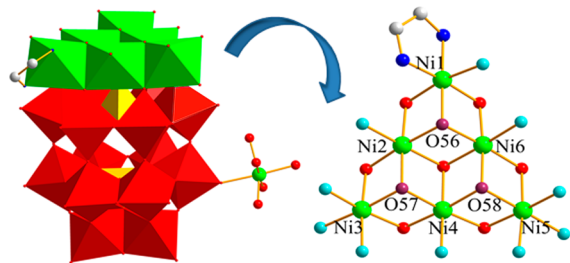
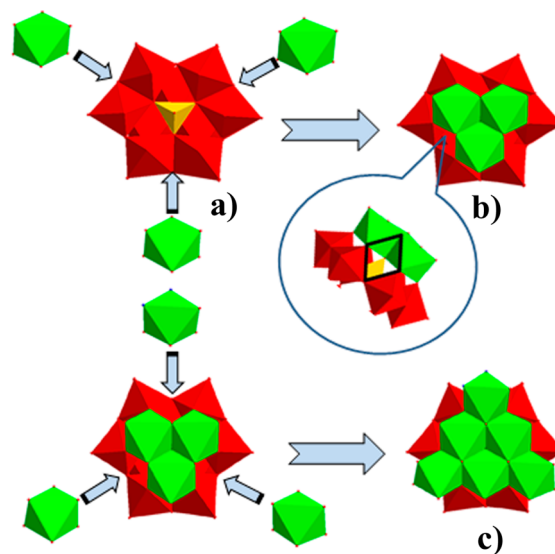


Figure 1. (a) The structure of compound **1**; water molecules are omitted for clarity. (b) The ball-and-stick representation of $\{Ni_6\}$ cluster in **1**. (color code: WO_6 , red polyhedron; NiO_6 or NiO_4N_2 , green polyhedron; PO_4 , golden polyhedron; Ni, green spheres; N, blue spheres; C, gray spheres; O atoms from P_2W_{15} , red spheres; O atoms from terminal water, light blue spheres; O atoms from hydroxyls, purple spheres).

$OH_3(H_2O)_9P_2W_{15}O_{56}]^{12-}$ (**1a**), half of a $[Ni(H_2O)_6]^{2+}$ cation, one en and 10 water molecules. The structure of **1a** could be described as follows: Three truncated cubanes ($\{Ni_3O_4\}$) formed a $[Ni_6(\mu_3-OH)_3]^{9+}$ cluster (abbreviated as $\{Ni_6\}$) by sharing not only one edge with each other but also a common μ_4-O (Figure S3, Supporting Information); then the $\{Ni_6\}$ cluster capped on the $[P_2W_{15}O_{56}]^{12-}$ polyanion to form compound **1**. Through careful observation, we found that the structure of **1** contains a $\beta-Ni_3P_2W_{15}$ unit, which has not been obtained up to now. Therefore, we carried on a detailed

research about the structure of compound **1**. During the research, we found that the $\beta-Ni_3P_2W_{15}$ unit has three relatively large rhombic windows through which the Ni^{2+} can attach to the $\{Ni_3\}$ cluster from the $\beta-Ni_3P_2W_{15}$ unit to form a $\{Ni_6\}$ cluster. We also investigated all the reported compounds that contain a $\{M_6\}$ cluster, finding that all of them contain a $\beta-M_3XW_9$ ($M = Ni, Cu, Co; X = P, Si$) unit with three relatively large rhombic windows when three exterior M-octahedron groups are removed^{49–57} (Figure S4, Supporting Information). Besides, the trilacunary polyanion $[P_2W_{15}O_{56}]^{12-}$ can capture three Ni^{2+} easily to form a saturated $\beta-Ni_3(\mu_3-OH)_3-(H_2O)_3P_2W_{15}O_{56}$ ($\beta-Ni_3P_2W_{15}$) unit. The pure inorganic $\{Ni_6\}$ cluster without POMs has not been obtained up to now. On the basis of the above description, we speculate that the formation of compound **1** may be as follows: First, three scattered Ni^{2+} were captured by the $[P_2W_{15}O_{56}]^{12-}$ polyanion to form a monomeric trisubstituted Dawson unit $\beta-Ni_3P_2W_{15}$. Then, another three scattered Ni^{2+} are attached to the $\beta-Ni_3P_2W_{15}$ unit to form a $\{Ni_6\}$ cluster substituted Dawson POM (Scheme 1).

Scheme 1. Possible Formation Process of Compound 1: (a) $P_2W_{15}O_{56}$, (b) $\beta-Ni_3(\mu_3-OH)_3(H_2O)_3P_2W_{15}O_{56}$ ($\beta-Ni_3P_2W_{15}$) Unit, (c) Top View of Compound **1**^a



^aWater molecules and en are omitted for clarity. Color code: WO_6 , red; PO_4 , golden; NiO_6 , green.

In the $\{Ni_6\}$ cluster (Figure 1b), the $[Ni_6(\mu_3-OH)_3]^{9+}$ triangle is composed of six Ni^{2+} ions and three hydroxyls, as well as stabilized by an en, and it also contains 10 terminal aqua ligands and seven O atoms from the $[P_2W_{15}O_{56}]^{12-}$ unit. The Ni^{2+} ions could be divided into three classes according to the coordination environments: Ni2, Ni4, Ni6; Ni3, Ni5; and Ni1. The Ni^{2+} ions located at the trivacant sites of $[P_2W_{15}O_{56}]^{12-}$ (Ni2/Ni4/Ni6) are coordinated with three O atoms from P_2W_{15} , two μ_3-O , and one O atom from water, and they fused together by edge-sharing to form a $\{Ni_3O_{13}\}$ cluster, which also can be described as a truncated cubane. The Ni^{2+} ions located at one vertex of the triangle (Ni1) is coordinated with two O from P_2W_{15} , one μ_3-O (O56), two N atoms from one en, and one O atom from water. The Ni^{2+} ions located at another two vertexes of the triangle (Ni3, Ni5) are coordinated with two O atoms from P_2W_{15} , one μ_3-O (O57) atom, and three O atoms

from water. They attach to the $\{\text{Ni}_3\text{O}_{13}\}$ cluster by edge-sharing to form a triangular $\{\text{Ni}_6\}$ cluster. Such a $\{\text{Ni}_6\}$ cluster is reported rarely in Dawson-type POMs up to now. Structurally, the $\{\text{Ni}_6\}$ cluster is different from the reported $\{\text{Ni}_6\}$ cluster. The $\{\text{Ni}_6\}$ cluster in **1** is stabilized by only one organic amine, whereas the number of the organic amine in the most reported $\{\text{Ni}_6\}$ cluster is two to three.^{49–54} Thus, the number of the terminal aqua ligands in **1** is more than that reported. To date, there is only one example of a $\{\text{Ni}_6\}$ cluster that contains 12 terminal aqua ligands that has been reported.⁵⁷ **1** has 10 terminal aqua ligands; to the best of our knowledge, **1** has the highest number of terminal aqua ligands in isolated transition-metal-substituted phosphotungstate. As a result, **1** is more easily substituted by some oxygen-containing ligands to form more novel 3D inorganic–organic hybrid compounds.⁵⁸ In addition, it is also a step forward for constructing a pure inorganic $\{\text{Ni}_6\}$ cluster without stabilization by an organic ligand.

Bond valence sum (BVS) calculations (Tables S1) reveal that the range of bond valences for the 10 terminal O atoms on Ni sites is 0.301–0.351, suggesting that all of them are diprotonation, while the bond valences of the three $\mu_3\text{-O}$ (O56, O57, O58) are 1.077, 1.094 and 1.08, respectively, indicating that they are monoprotonation. To balance the charges of **1**, two protons are added. The two protons cannot be located crystallographically and are supposed to be delocalized over the entire structure; this is common in polyoxometalates.⁵⁹

The synthetic procedure of compound **2** was the same as that of **1**, except that the en was replaced with dap, and added appropriate succinic acid to the above system. Single-crystal structural analysis reveals that **2** crystallizes in the space group C2/c. The structure of **2** is based on **1**, except that the $\{\text{Ni}_6\}$ cluster in **2** is stabilized by two dap and one en. The asymmetric unit of **2** (Figure S5, Supporting Information) contains a dimeric secondary building unit (SBU) $\{\text{Ni}_6(\text{dap})_2(\text{en})(\text{P}_2\text{W}_{15})(\text{H}_2\text{O})_2\}_2$ linked by $[\text{Ni}(\text{dap})(\text{H}_2\text{O})_2]$, one succinic acid unit, two CH_3COO^- units, as well as an isolated $[\text{Ni}(\text{dap})_2]^{2+}$ cation. As shown in Figure 2a, the $\{\text{Ni}_6\text{P}_2\text{W}_{15}\}$ unit links with each other through a $\text{W}=\text{O}-\text{Ni}$ linkage to form infinite 1D chain $\{\text{Ni}_6\text{P}_2\text{W}_{15}\}_\infty$ SBUs along the *b* axis. Furthermore, the SBUs are linked interlaced by succinic

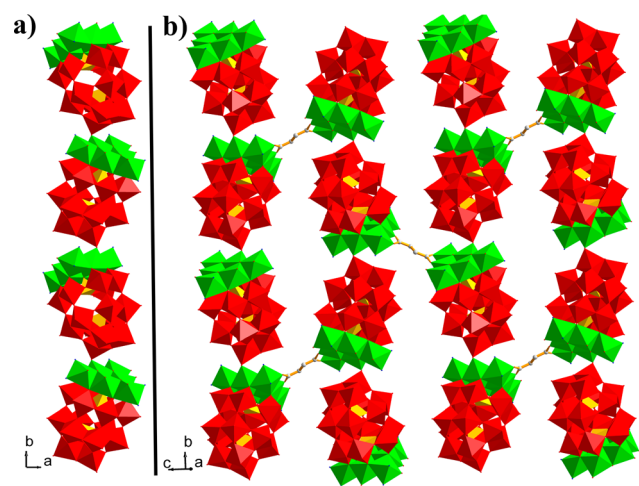


Figure 2. (a) Views of infinite $\{\text{Ni}_6\text{P}_2\text{W}_{15}\}_\infty$ chain along the *b* axis. (b) The 2D layer in **2**. The amine ligands are omitted for clarity.

acid to form a 2D layer (Figure 2b), and then the 2D layer is bridged by $[\text{Ni}(\text{dap})(\text{H}_2\text{O})_2]$ through O–Ni–O to form a 3D structure (Figure S6, Supporting Information). To better comprehend the 3D structure, Figure S7 (Supporting Information) shows the 2D structural pictures viewed along the *c* axes. It is noted that the $\{\text{Ni}_6\text{P}_2\text{W}_{15}\}$ unit in **2** is different from **1**, and the $\{\text{Ni}_6\text{P}_2\text{W}_{15}\}$ unit in **1** is stabilized by only one en. However, the unit in **2** is stabilized by two dap as well as an en (Figure S8, Supporting Information). We think that the superfluous en originates probably from the impurities of dap. Furthermore, the $\{\text{Ni}_6\text{P}_2\text{W}_{15}\}$ unit in **2** is also stabilized by a CH_3COO^- unit and half of succinic acid unit through which the $\{\text{Ni}_6\text{P}_2\text{W}_{15}\}$ unit was linked into the multidimensional structure. BVS calculations for **2** show that all the W atoms are in the +6 oxidation state, and the Ni atoms are in the +2 oxidation state. In addition, there are also three monoprotonated oxygens in each $\{\text{Ni}_6\text{P}_2\text{W}_{15}\}$ unit; the BVS ranges for these oxygens are 1.101–1.167. The bond valence of the only one terminal oxygen is 0.262, suggesting diprotonation.

Thermal Stability Analysis. The thermal stability of the two compounds was investigated under a N_2 atmosphere with a heating rate of $10\text{ }^\circ\text{C}/\text{min}$ from 30 to $800\text{ }^\circ\text{C}$ (Figure S9, Supporting Information). The TG curve of **1** shows three steps of weight loss in the range of 30– $800\text{ }^\circ\text{C}$. The first weight loss is 3.87% (calc. 4.10%) from 30 to $210\text{ }^\circ\text{C}$, assigned to the release of 10 lattice water molecules, followed by the loss of 6.89% (calc. 6.98%) from 210 to $573\text{ }^\circ\text{C}$ corresponding to the removal of 15 coordinated water molecules and the dehydration of three hydroxyl groups. The last weight loss is 1.30% (calc. 1.83%) from 573 to $800\text{ }^\circ\text{C}$, which is attributed to the decomposition of one en. For **2**, the TG curve shows four steps of weight loss in the range of 30– $800\text{ }^\circ\text{C}$. The first weight loss is 5.53% (calc. 5.20%) from 30 to $335\text{ }^\circ\text{C}$, assigned to the release of 15 lattice water molecules; the second weight loss is 5.32% (calc. 4.80%) from 335 to $410\text{ }^\circ\text{C}$, which can be ascribed to the release of four coordinated water molecules, the decomposition of three hydroxyl groups and carboxylate ligands. The last two steps of weight loss is 9.17% (calc. 8.99%) occurring from 410 to $800\text{ }^\circ\text{C}$, which can be attributed to the decomposition of the organic amine. These observations are also in compliance with elemental analysis. The X-ray powder diffraction patterns of **2** after being heated at $120\text{ }^\circ\text{C}$ and as-synthesized are identical except that the intensity show some differences (Figure S2), revealing that **2** has good thermal stability.

Magnetic Measurements. The magnetic susceptibility of **1** was measured over the range of 2– 300 K . The plots of molar magnetic susceptibility χ_M and $\chi_M T$ versus *T* of **1** under a constant magnetic field of 1000 Oe are shown in Figure 3. The χ_M value of **1** is $0.03134\text{ emu mol}^{-1}$ at 300 K ; upon cooling, the χ_M value of **1** slowly increases to $0.67125\text{ emu mol}^{-1}$ at 25 K , and then quickly reaches a maximum value of $7.298\text{ emu mol}^{-1}$ at 2 K . The value of $\chi_M T$ at 300 K is $9.40\text{ emu mol}^{-1}\text{ K}$, which is corresponding to six uncoupled high-spin Ni^{2+} ions with $g > 2$, $S = 1$. As the temperature decreases, the value of $\chi_M T$ increases to a maximum of $18.054\text{ emu mol}^{-1}\text{ K}$ at 11 K . This magnetic behavior of the $\chi_M T$ versus *T* plots for **1** shows the presence of the intramolecular ferromagnetic coupling interactions between adjacent Ni^{2+} centers. Then, the value of $\chi_M T$ decreases sharply below 11 K ; this may be dominantly assigned to the presence of zero-field splitting (ZFS). In brief, the behavior suggests that there exist overall ferromagnetic interactions with the presence of ZFS for Ni^{2+} ions. The

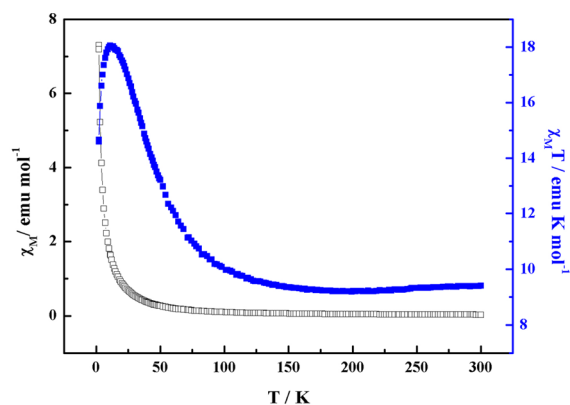


Figure 3. Temperature dependence of the molar magnetic susceptibility χ_M (open square) and the product of the molar magnetic susceptibility and temperature $\chi_M T$ (blue square) for **1** between 2 and 300 K.

temperature dependence of the reciprocal susceptibilities ($1/\chi_M$) obeys the Curie–Weiss law above 30 K for **1** and with a positive Weiss constant $\theta = 12.97$ K (Figure S10, Supporting Information), which further support the presence of overall ferromagnetic coupling between the Ni^{2+} ions in **1**. The magnetic property of **2** is similar to that of **1** (Figure S11, Supporting Information), so we will not describe it further. Such magnetic characteristics are consistent with those reported in previous studies.^{49,50}

Adsorption Properties. The adsorption isotherms of water, methanol, and ethanol for **2** were measured at 25 °C. The sample of **2** was heated at 120 °C for 5 h under a vacuum to remove the guest solvent molecules before the measurements. As shown in Figure 4, with the increasing of relative

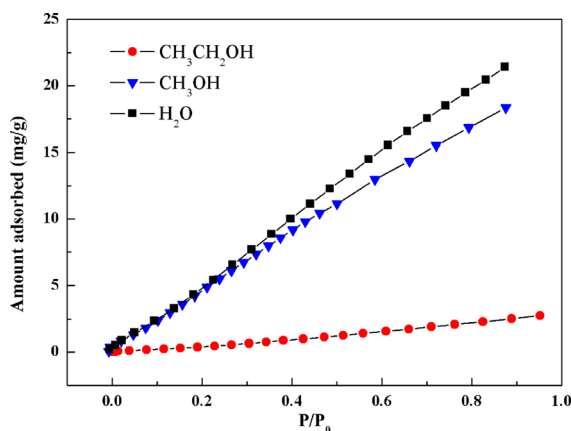


Figure 4. Water (black square), methanol (blue triangle), and ethanol (red circle) adsorption isotherms of **2** at 25 °C.

pressure (P/P_0), the distinction of the adsorption amount of water and ethanol is more obvious. The amount adsorbed for water and ethanol was 21.4 and 2.7 mg/g, respectively, when the relative pressure reached to 0.95, which is equivalent to the adsorption of 6.3 molecules of water and 0.3 molecules of ethanol per formula unit. As we all know, water and ethanol are easy to form an azeotrope and difficult to separate; the adsorption isotherms indicated that **2** can selectively adsorb water molecules over ethanol to make them separate. In the same way, **2** can also adsorb methanol molecules selectively to remove some methanol molecules mixed in industrial alcohol.

CONCLUSIONS

In summary, two $\{\text{Ni}_6\}$ cluster-containing inorganic–organic hybrid compounds based on a $\{\text{P}_2\text{W}_{15}\}$ unit have been successfully synthesized under hydrothermal conditions, and characterized by IR spectra, X-ray diffraction, and magnetic properties. Magnetic measurements illustrate that both of them have the overall ferromagnetic coupling between the Ni^{2+} ions. Structural analyses indicate that **1** contains a $\{\text{Ni}_6\}$ cluster stabilized by only one en, and there are more terminal aqua water ligands in the $\{\text{Ni}_6\}$ cluster that could be substituted easily, so it is beneficial in making an extended structure of compound **1**. **2** is a 3D hybrid compound linked by succinic acid; it exhibits the selective adsorption abilities to water and ethanol molecules, which is meaningful in the separation of water and ethanol. It also can selectively adsorb methanol over ethanol, which will have potential application in removing of the methanol mixed in industrial alcohol. Besides, the successful synthesis of these two compounds has laid the groundwork for the preparation of the trisubstituted Dawson $\text{Ni}_3\text{P}_2\text{W}_{15}$ unit. The future work is underway on isolating the monomeric trisubstituted Dawson $\text{M}_3\text{P}_2\text{W}_{15}$ units.

ASSOCIATED CONTENT

Supporting Information

The IR spectra, PXRD patterns, TG curves, magnetic properties, the additional structural figures, and the table of the BVS calculation result of the oxygen atoms for **1** (Table S1). This material is available free of charge via the Internet at <http://pubs.acs.org>.

AUTHOR INFORMATION

Corresponding Authors

*E-mail: liusx@nenu.edu.cn (S.L.).

*E-mail: ygy@fjirsm.ac.cn (G.Y.).

Notes

The authors declare no competing financial interest.

ACKNOWLEDGMENTS

This work was supported by the National Natural Science Foundation of China (Grants 21171032, 21371029, and 21231002), the Key Technologies R&D Program of Jilin Province of China (Grant 20130206079SF), and the Open Research Fund of the State Key Laboratory of Inorganic Synthesis and Preparative Chemistry (Jilin University, Grant 2015-01).

REFERENCES

- Haag, R. *Angew. Chem., Int. Ed.* **2004**, *43*, 278–282.
- Griset, A. P.; Walpole, J.; Liu, R.; Gaffey, A.; Colson, Y. L.; Grinstaff, M. W. *J. Am. Chem. Soc.* **2009**, *131*, 2469–2471.
- Kanie, K.; Sugimoto, T. *J. Am. Chem. Soc.* **2003**, *125*, 10518–10519.
- Hoffmann, F.; Cornelius, M.; Morell, J.; Fröba, M. *Angew. Chem., Int. Ed.* **2006**, *45*, 3216–3251.
- Proust, A.; Thouveno, R.; Gouzerh, P. *Chem. Commun.* **2008**, 1837–1852.
- Wei, M. L.; Sun, J. J.; Duan, X. Y. *Eur. J. Inorg. Chem.* **2014**, 345–351.
- Corma, A.; Díaz, U.; García, T.; Sastre, G.; Velty, A. *J. Am. Chem. Soc.* **2010**, *132*, 15011–15021.
- Cariati, E.; Macchi, R.; Roberto, D.; Ugo, R.; Galli, S.; Casati, N.; Macchi, P.; Sironi, A.; Bogani, L.; Caneschi, A.; Gatteschi, D. *J. Am. Chem. Soc.* **2007**, *129*, 9410–9420.

- (9) Liu, J. L.; Yan, B.; Guo, L. *Eur. J. Inorg. Chem.* **2010**, 2290–2296.
- (10) Hagrman, D.; Hagrman, P. J.; Zubieta, J. *Angew. Chem., Int. Ed.* **1999**, *38*, 3165–3168.
- (11) Masciocchi, N.; Galli, S.; Colombo, V.; Maspero, A.; Palmisano, G.; Seyyedi, B.; Lamberti, C.; Bordiga, S. *J. Am. Chem. Soc.* **2010**, *132*, 7902–7904.
- (12) Liu, C. M.; Xiong, R. G.; Zhang, D. Q.; Zhu, D. B. *J. Am. Chem. Soc.* **2010**, *132*, 4044–4045.
- (13) Pope, M. T.; Müller, A. *Angew. Chem., Int. Ed. Engl.* **1991**, *30*, 34–48.
- (14) Hasenknopf, B.; Micoine, K.; Lacôte, E.; Thorimbert, S.; Malacria, M.; Thouvenot, R. *Eur. J. Inorg. Chem.* **2008**, *32*, 5001–5013.
- (15) Kortz, U.; Müller, A.; Van Slageren, J.; Schnack, J.; Dalal, N. S.; Dressel, M. *Coord. Chem. Rev.* **2009**, *253*, 2315–2327.
- (16) Long, D. L.; Tsunashima, R.; Cronin, L. *Angew. Chem., Int. Ed.* **2010**, *49*, 1736–1758.
- (17) Long, D. L.; Burkholder, E.; Cronin, L. *Chem. Soc. Rev.* **2007**, *36*, 105–121.
- (18) Raj, C.; Swales, C.; Guillet, A.; Devillers, M.; Nysten, B.; Gaigneaux, E. M. *Langmuir* **2013**, *29*, 4388–4395.
- (19) Nomiya, K.; Yoshida, T.; Sakai, Y.; Nanba, A.; Tsuruta, S. *Inorg. Chem.* **2010**, *49*, 8247–8254.
- (20) Uehara, K.; Kasai, K.; Mizuno, N. *Inorg. Chem.* **2007**, *46*, 2563–2570.
- (21) Han, Z.; Wang, Y.; Song, X.; Zhai, X.; Hu, C. *Eur. J. Inorg. Chem.* **2011**, 3082–3090.
- (22) Bassil, B. S.; Mal, S. S.; Dickman, M. H.; Kortz, U.; Oelrich, H.; Walder, L. *J. Am. Chem. Soc.* **2008**, *130*, 6696–6697.
- (23) Niu, J. Y.; Wang, Z. L.; Wang, J. P. *J. Solid State Chem.* **2004**, *177*, 3411–3417.
- (24) Kato, C. N.; Shinohara, A.; Hayashi, K.; Nomiya, K. *Inorg. Chem.* **2006**, *45*, 8108–8119.
- (25) Bi, L. H.; Kortz, U.; Keita, B.; Nadjó, L.; Borrmann, H. *Inorg. Chem.* **2004**, *43*, 8367–8372.
- (26) Ruhlmann, L.; Nadjó, L.; Canny, J.; Contant, R.; Thouvenot, R. *Eur. J. Inorg. Chem.* **2002**, 975–986.
- (27) Finke, R. G.; Rapko, B.; Weakley, T. J. *R. Inorg. Chem.* **1989**, *28*, 1573–1579.
- (28) Bassil, B. S.; Dickman, M. H.; Kortz, U. *Inorg. Chem.* **2006**, *45*, 2394–2396.
- (29) Kortz, U.; Jeannin, Y. P.; Tézé, A.; Hervé, G.; Lsber, S. *Inorg. Chem.* **1999**, *38*, 3670–3675.
- (30) Nellutla, S.; van Tol, J.; Dalal, N. S.; Bi, L.-H.; Kortz, U.; Keita, B.; Nadjó, L.; Khitrov, G. A.; Marshall, A. G. *Inorg. Chem.* **2005**, *44*, 9795–9806.
- (31) Zheng, S. T.; Yang, G. Y. *Chem. Soc. Rev.* **2012**, *41*, 7623–7646.
- (32) Hagrman, P. J.; Hagrman, D.; Zubieta, J. *Angew. Chem., Int. Ed.* **1999**, *38*, 2638–2684.
- (33) Hill, C. L. *Chem. Rev.* **1998**, *98*, 1–2.
- (34) Long, D. L.; Burkholder, E.; Cronin, L. *Chem. Soc. Rev.* **2007**, *36*, 105–121.
- (35) Hao, J.; Xia, Y.; Wang, L. S.; Ruhlmann, L.; Zhu, Y. L.; Li, Q.; Yin, P. C.; Wei, Y. G.; Guo, H. Y. *Angew. Chem., Int. Ed.* **2008**, *47*, 2626–2630.
- (36) Bassil, B. S.; Dickman, M. H.; Römer, I.; Kammer, B.; Kortz, U. *Angew. Chem., Int. Ed.* **2007**, *46*, 6192–6195.
- (37) Kurth, D. G.; Lehmann, P.; Volkmer, D.; Cölfen, H.; Koop, M. J.; Müller, A.; Chesne, A. D. *Chem.—Eur. J.* **2000**, *6*, 385–393.
- (38) Li, H.; Sun, H.; Qi, W.; Xu, M.; Wu, L. *Angew. Chem., Int. Ed.* **2007**, *46*, 1300–1303.
- (39) Ibrahim, M.; Lan, Y.; Bassil, B. S.; Xiang, Y.; Suchopar, A.; Powell, A. K.; Kortz, U. *Angew. Chem., Int. Ed.* **2011**, *50*, 4708–4711.
- (40) Lydon, C.; Sabi, M. M.; Symes, M. D.; Long, D. L.; Murrie, M.; Yoshii, S.; Nojiri, H.; Cronin, L. *Chem. Commun.* **2012**, *48*, 9819–9821.
- (41) Zhang, Z.; Wang, E.; Qi, Y.; Li, Y.; Mao, B.; Su, Z. *Cryst. Growth Des.* **2007**, *7*, 1305–1311.
- (42) Clemente-Juan, J. M.; Coronado, E.; Galán-Mascarós, J. R.; Gómez-García, C. J. *Inorg. Chem.* **1999**, *38*, 55–63.
- (43) Ibrahim, M.; Xiang, Y.; Bassil, B. S.; Lan, Y.; Powell, A. K.; Oliveira, P.; Keita, B.; Kortz, U. *Inorg. Chem.* **2013**, *52*, 8399–8408.
- (44) Mal, S. S.; Bassil, B. S.; Ibrahim, M.; Nellutla, S.; Tol, J.; Dalal, N. S.; Fernández, J. A.; López, X.; Poblet, J. M.; Biboum, R. N.; Keita, B.; Kortz, U. *Inorg. Chem.* **2009**, *48*, 11636–11645.
- (45) Zhang, J.; Song, Y. F.; Cronin, L.; Liu, T. *J. Am. Chem. Soc.* **2008**, *130*, 14408–14409.
- (46) Finke, R.; Droege, M. W.; Domaille, P. J. *Inorg. Chem.* **1987**, *26*, 3886–3896.
- (47) Henry, N. F. M.; Lonsdale, K., Eds. *International Tables for X-ray Crystallography*; Kynoch Press: Birmingham, U. K., 1952.
- (48) Sheldrick, G. M. *SHELXS-97: Program for the Refinement of Crystal Structure*; University of Göttingen: Göttingen, Germany, 1997.
- (49) Zhao, J. W.; Jia, H. P.; Zhang, J.; Zheng, S. T.; Yang, G. Y. *Chem.—Eur. J.* **2007**, *13*, 10030–10045.
- (50) Liu, Y. C.; Fu, C. H.; Zheng, S. T.; Zhao, J. W.; Yang, G. Y. *Dalton Trans.* **2013**, *42*, 16676–16679.
- (51) Zheng, Y. Y.; Wen, R.; Kong, X. J.; Long, L. S.; Huang, R. B.; Zheng, L. S. *Dalton Trans.* **2012**, *41*, 9871–9875.
- (52) Zhao, J. W.; Zhang, J.; Song, Y.; Zheng, S. T.; Yang, G. Y. *Eur. J. Inorg. Chem.* **2008**, 3809–3819.
- (53) Zheng, S. T.; Yuan, D. Q.; Jia, H. P.; Yang, G. Y. *Chem. Commun.* **2007**, *18*, 1858–1860.
- (54) Liu, X. X.; Wang, X. L.; Yang, G. S.; Yuan, G.; Li, L. J.; Shao, K. Z.; Su, Z. M.; Xie, H. M. *Inorg. Chem. Commun.* **2012**, *23*, 21–24.
- (55) Wang, X. L.; Liu, X. J.; Tian, A. X.; Ying, J.; Lin, H. Y.; Liu, G. C.; Gao, Q. *Dalton Trans.* **2012**, *41*, 9587–9589.
- (56) Li, B.; Zhao, J. W.; Zheng, S. T.; Yang, G. Y. *Inorg. Chem.* **2009**, *48*, 8294–8303.
- (57) Yang, L.; Huo, Y.; Niu, J. Y. *Dalton Trans.* **2013**, *42*, 364–367.
- (58) Zheng, S. T.; Zhang, J.; Yang, G. Y. *Angew. Chem., Int. Ed.* **2008**, *47*, 3909–3913.
- (59) Zheng, S. T.; Zhang, J.; Clemente-Juan, J. M.; Yuan, D. Q.; Yang, G. Y. *Angew. Chem., Int. Ed.* **2009**, *48*, 7176–7179.